JOURNAL OF MATERIALS SCIENCE **34** (1999) 53–58

Comparative effects of the hydrogen and nitrogen gas treatment and re-calcination (GTR) routes on the composition, microstructure, and magnetic properties of conventionally synthesized Sr–hexaferrite

S. A. S. EBRAHIMI*, C. B. PONTON, I. R. HARRIS
School of Metallurgy and Materials, The University of Birmingham, Edgbaston, Birmingham, B15 2TT, UK

A. KIANVASH
Department of Ceramic Engineering, Faculty of Engineering, The University of Tabriz, Tabriz 51 664, Iran

Optimized static hydrogen treated and recalcined (HTR) and static nitrogen treated and recalcined (NTR) Sr–hexaferrite powders synthesized conventionally in-house are compared with one another. The phase identification studies and lattice parameter measurements showed first that the Sr–hexaferrite decomposed, forming iron oxide (Fe_2O_3), which was then reduced during the static hydrogen or nitrogen treatment, and, second, that the hexaferrite phase was recovered albeit with a small change in the composition (as indicated by the lattice spacings) after the re-calcination treatment in static air. These effects were more pronounced in the hydrogen process than in the nitrogen process. The main effect of this gas-treatment and re-calcination (GTR) process on the microstructure of the Sr–hexaferrite was the transformation of the single-crystal particles into particles with a very fine sub-grain structure during the gas treatment, which resulted in the formation of polycrystalline hexaferrite particles with a much finer grain size during subsequent recalcination, compared to that of the initial hexaferrite powder. This finer structure was responsible for the higher coercivities observed after re-calcination. With regard to the hydrogen and nitrogen processes, the former resulted in a higher degree of oxide reduction and hence a higher coercivity on re-calcination. The coercivity of the initial Sr–hexaferrite increased from 310 kA/m (3.9 kOe) to ~400 kA/m (5 kOe) after HTR and to 342 kA/m (4.3 kOe) after NTR. The initial magnetization behavior was also different for the HTR- and NTR-processed powders, with the former exhibiting behavior characteristic of single domains. This was consistent with the grain size being significantly less than the single-domain size (~1μ).

1. Introduction

A new magnetic properties modification technique involving the heat treatment of hexaferrites in the presence of hydrogen, nitrogen, or carbon has been patented and reported for commercial and hydrothermally produced Sr–hexaferrite materials [1, 2]. Further investigative work on the effect of this technique on in-house conventionally synthesized Sr–hexaferrite has since been conducted [3]. Low coercivities can be achieved by heat treatment in gaseous atmospheres (i.e., hydrogen or nitrogen treatment), while high coercivities can be obtained by a subsequent re-calcination process. Subsequently, optimization of the hydrogen and nitrogen gas treatment, as well as the concomitant re-calcination processes, was undertaken [4, 5]. The optimum hydrogen process, i.e., hydrogen treatment and re-calcination (HTR) was established as hydrogenation at 700 °C under an initial static gas pressure of 1.3 bar for 1 h, followed by re-calcination in static air at 1000 °C for 1 h. For the nitrogen process (i.e., NTR), it was nitrogenation at 950 °C under an initial pressure of 1 bar for 5 h, followed by re-calcination at 1000 °C for 1 h. The phase transformations and changes in magnetic properties occurring during the dynamic hydrogenation

* Also Department of Metallurgy, Faculty of Engineering, Tehran University, P.O. Box 11365-4563, Tehran, Iran.

and subsequent re-calcination treatment in static air of commercially sourced Sr–hexaferrite will be reported elsewhere [6].

In this work, the characteristics of the optimum hydrogen–processed Sr–hexaferrite powder are compared with those of the optimum nitrogen–processed material. Thus, the lattice parameters, phase constitution, microstructure, and magnetic properties of these powders at different stages in the gas-treatment and re-calcination (GTR) process were compared.

2. Experimental procedure

The starting material was M-type strontium hexaferrite produced conventionally in-house from strontium carbonate and iron oxide (α-Fe_2O_3) without using additives. The details of production of the hexaferrite powder have been described previously [3, 4]. The gas treatment was carried out in a static atmosphere. The amount of powder in each batch was 4 g. The optimized hydrogen treatment consisted of heating the powder at a rate of 5 °C/min to 700 °C under an initial gas pressure of 1.3 bar, dwelling for 1 h, and then cooling at the same rate in a resistance-heated vacuum tube furnace. In the optimized nitrogen treatment, the temperature, time, and initial gas pressure were 950 °C, 5 h, and 1 bar, respectively. The optimized re-calcination process (for both hydrogen and nitrogen gas treatment) consisted of heating in static atmosphere to 1000 °C, dwelling for 1 h, and then cooling in a resistance-heated muffle furnace. The heating and cooling rates were 5 °C/min and 10 °C/min, respectively. The magnetic properties were measured at room temperature using a vibrating sample magnetometer (VSM) operating up to a maximum field of 1100 kA/m. The degree of magnetization at this field strength is referred to as maximum magnetization (M_m) in this work. The majority of the VSM samples were mixed with a molten wax but were not magnetically aligned, making the samples magnetically isotropic. This aspect of the work requires further investigation. On applying a field, there was no evidence of anisotropy in the treated powders. An X-ray diffractometer (XRD) (CoK_α radiation) was used for the phase identification and lattice parameter measurements. Thermal magnetic analysis (TMA) was performed on a Sucksmith balance. The particle microstructures and morphologies, as well as the particle and sub-grain sizes, were studied using a Hitachi S-4000 FEG high-resolution scanning electron microscope (HRSEM).

3. Results and discussion

3.1. Phase transformations

During the hydrogenation and nitrogenation treatments, the hexaferrite phase decomposed into $Sr_7Fe_{10}O_{22}$ and Fe_2O_3, and then the Fe_2O_3 was reduced. In Fig. 1, the XRD traces of the samples hydrogenated and nitrogenated optimally are compared to those of the initial powder. It can be seen that, in the hydrogenated sample (Fig. 1b), the peaks due to the Sr–hexaferrite are completely absent, and the reduction of Fe_2O_3 has resulted in the formation of Fe [7–9]. However, traces of FeO

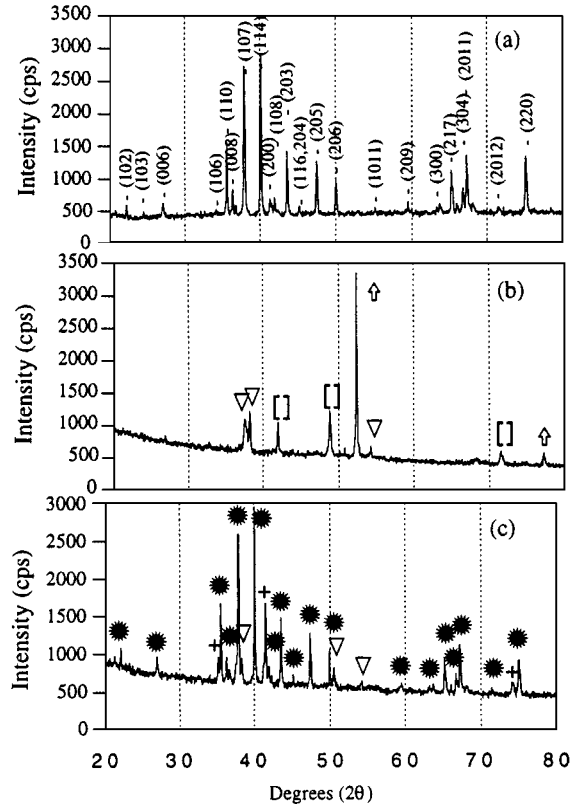

Figure 1 XRD traces of (a) initial; (b) optimally hydrogenated; and (c) optimally nitrogenated powders (⇧ = Fe, ∇ = $Sr_7Fe_{10}O_{22}$, [] = FeO, ✸ Sr–hexaferrite, + = Fe_3O_4). The Sr–hexaferrite indices are shown in (a).

can also be distinguished [10]. In the nitrogenated sample (Fig. 1c), the Sr–hexaferrite peaks are still present, and the extent of Fe_2O_3 reduction was limited to the formation of Fe_3O_4, even though the optimum treatment temperature and time are greater than for the hydrogenated powder [11]. No evidence of Fe or even FeO was obtained. This means that, as expected, the reduction process occurs to a much greater degree in the H-treatment than in the N-treatment.

In Fig. 2, the TMA patterns for the samples optimally hydrogenated and nitrogenated are compared to that of the initial powder. Fig. 2a shows the strontium hexaferrite curve with a slope change (i.e., trough in the dM/dT curve) at 440 °C (± 20 °C), which is close to the reported Curie point of this phase of 470 ± 10 °C [12]. Another prominent slope change at around 130 °C is due to the magnetic contribution of the sample holder, which acts as an internal calibration. It can be seen that, after the hydrogenation process (Fig. 2b), the hexaferrite phase was completely absent, whereas after nitrogenation, the trough due to the Sr–hexaferrite was still distinguishable. These observations are entirely consistent with the XRD studies.

During the re-calcination treatment that followed both the hydrogenation and nitrogenation processes, the hexaferrite phase re-formed by an oxidation reaction. Fig. 3b and c show the XRD traces of the optimum re-calcined powders after hydrogenation and nitrogenation, respectively, confirming that after re-calcination, only the XRD pattern for the Sr–hexaferrite phase could be observed. These findings are consistent with

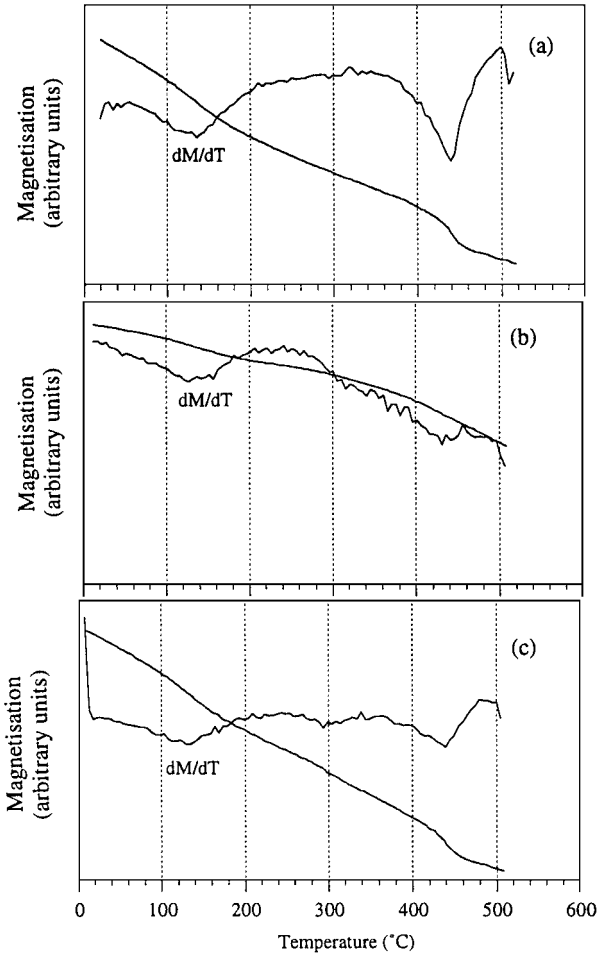

Figure 2 TMA and dM/dT as functions of temperature for (a) initial; (b) optimally hydrogenated; and (c) optimally nitrogenated powders.

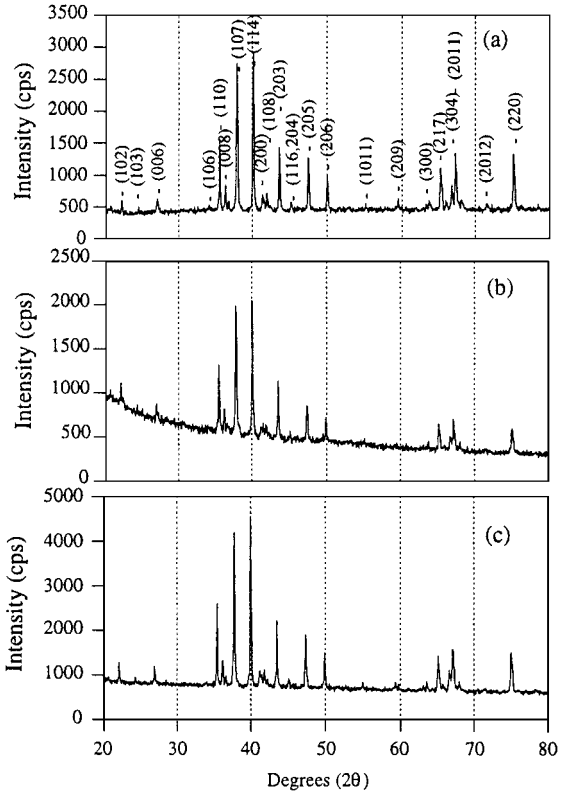

Figure 3 XRD traces of (a) initial powder; (b) optimally hydrogenated and re-calcined powders; and (c) optimally nitrogenated and re-calcined powders.

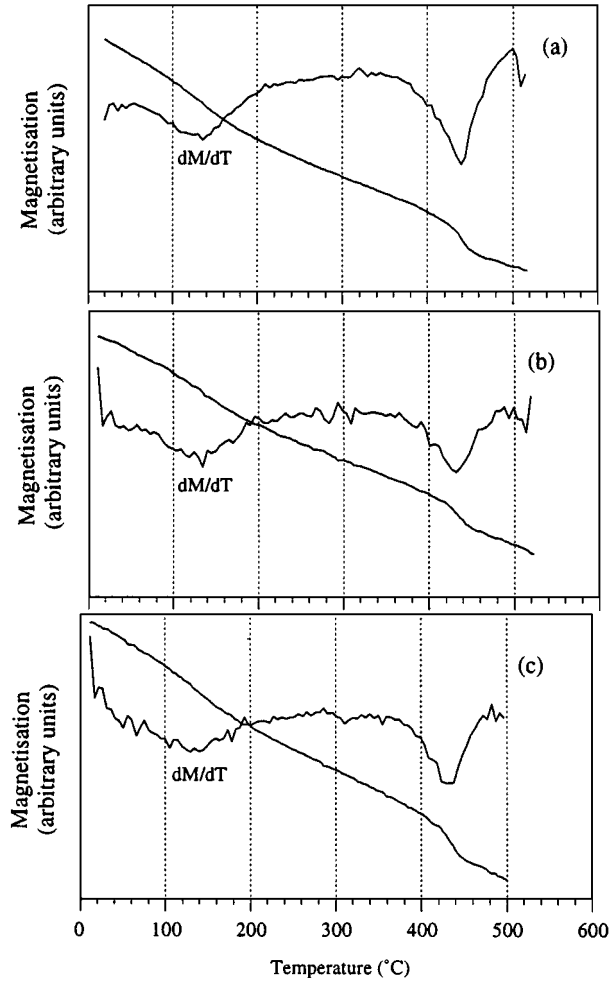

Figure 4 TMA and dM/dT as functions of temperature for (a) initial; (b) optimally hydrogenated and re-calcined; and (c) optimally nitrogenated and re-calcined powders.

the TMA patterns for these two powders, presented in Fig. 4b and c, which clearly show the Sr–hexaferrite trough in both samples after re-calcination. Both the TMA plots indicate that the Curie temperature of the re-formed hexaferrite was around 10 °C lower than that of the initial powder, which indicates a possible composition shift after HTR and NTR processes.

The lattice parameter measurements for re-calcined Sr–hexaferrite powder samples after the HTR and NTR processes are compared to those of the initial powder in Table I. It can be seen that after both processes, the lattice parameters had changed significantly, with the bigger change being observed in the case of HTR. The c-spacings had increased and a-spacings

TABLE I Measured lattice parameters for the optimally produced initial, HTR processed, and NTR processed powders

Sample	*a* (±0.0001 Å)	*c* (±0.0001 Å)
Initial	5.8877	23.0348
Hydrogenated and Re-calcined	5.8810	23.1088
Nitrogenated and Re-calcined	5.8825	23.0594

decreased. These changes in the lattice parameters suggest a change in the composition, probably in the oxygen content, and are consistent with the small changes observed in the Curie temperature. The bigger changes observed in the case of HTR are consistent with the greater degree of reduction and complete decomposition of the hexaferrite on hydrogenation.

3.2. Microstructure

The microstructural features of the initial powder are compared with those of the optimally hydrogenated and nitrogenated materials in Figs 5 to 7. The comparison between the microstructure of the optimum powder produced by hydrogenation (Fig. 6) with that of the optimum powder produced by nitrogenation (Fig. 7) reveals that the transformation of the initial single-crystal particles into particles comprising very fine sub-grains, which occurs during the gas treatments, is more extensive as a result of hydrogenation than nitrogenation. While Fig. 6 exhibits an extensive number of fine sub-grains in each particle, Fig. 7 shows changes at the edges

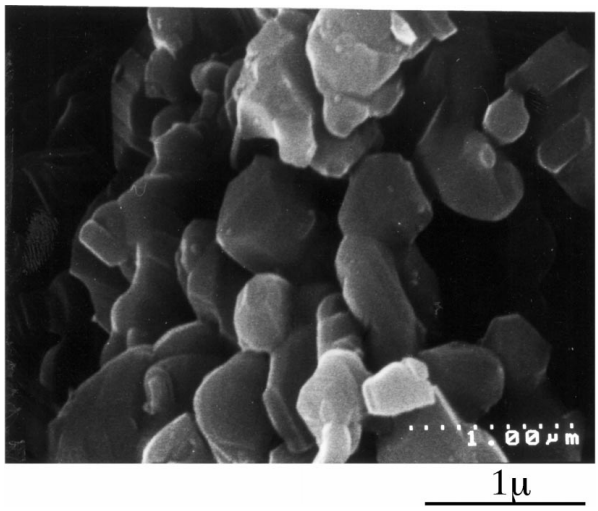

Figure 5 HRSEM micrograph of the initial powder showing the particles to have smooth surfaces and sharp edges.

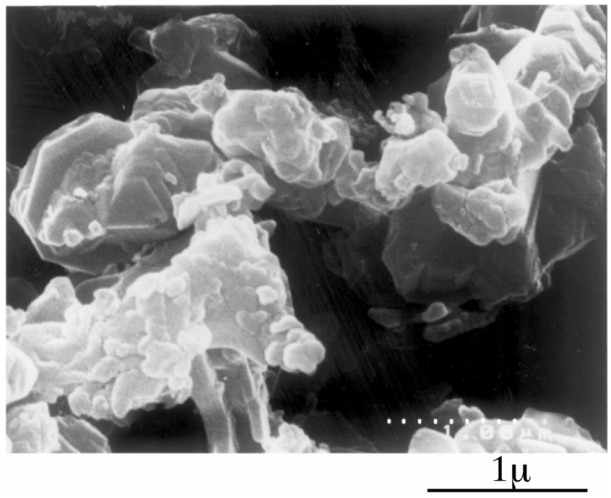

Figure 6 HRSEM micrograph of the conventionally synthesized Sr–hexaferrite powder after hydrogenation under optimum conditions (700 °C for 1 h under an initial gas pressure of 1.3 bar).

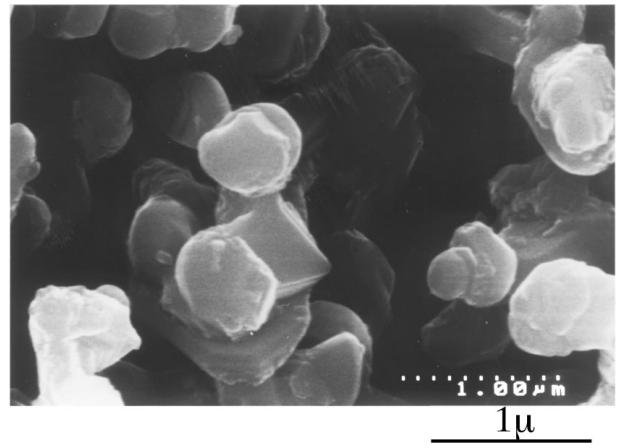

Figure 7 HRSEM micrograph of the conventionally synthesized Sr–hexaferrite powder after nitrogenation under optimum conditions (950 °C for 5 h under an initial gas pressure of 1 bar), showing the uneven grain edges.

of some of the initial particles and the appearance of only a limited number of fine sub-grains in them. This is consistent with the persistence of the hexaferrite phase in the nitrogenated powder.

The finer structure resulting from the gas treatments is due to the formation of fine sub-grains, leading to a finer structure after re-calcination. It can be observed clearly by comparing the powder re-calcined optimally after hydrogenation (Fig. 8) with the powder re-calcined optimally after nitrogenation (Fig. 9), that the finer structure is exhibited by the former.

3.3. Magnetic properties

The comparative magnetization curves of the Sr–hexaferrite powder before gas treatment and after optimum hydrogenation and nitrogenation are shown in Fig. 10. It can be seen that after the optimum hydrogenation treatment, there is a dramatic decrease in the remanence and coercivity and a drastic increase in the maximum magnetization. These effects can be attributed to the reduction of the iron oxide and the formation of iron, which is magnetically soft. After nitrogenation, these

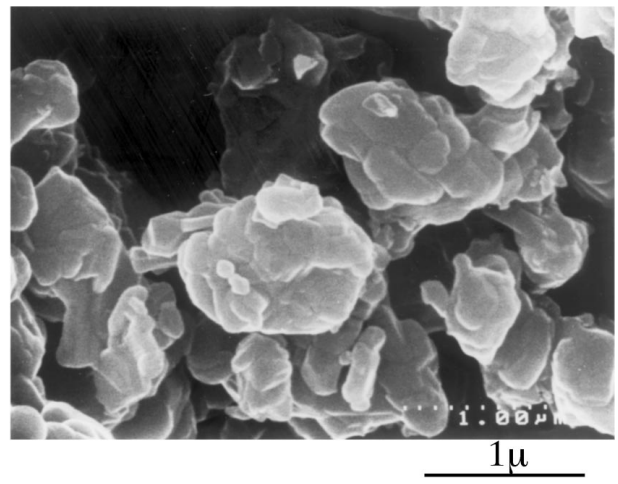

Figure 8 HRSEM micrograph of the conventionally synthesized Sr–hexaferrite powder after being optimally HTR processed.

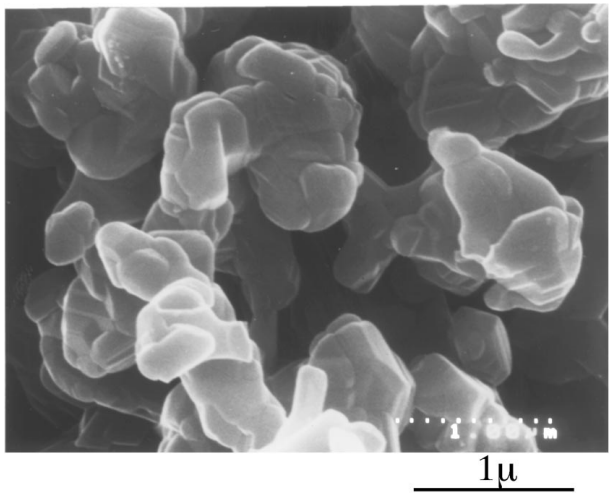

Figure 9 HRSEM micrograph of the conventionally synthesized Sr–hexaferrite powder after being optimally NTR processed.

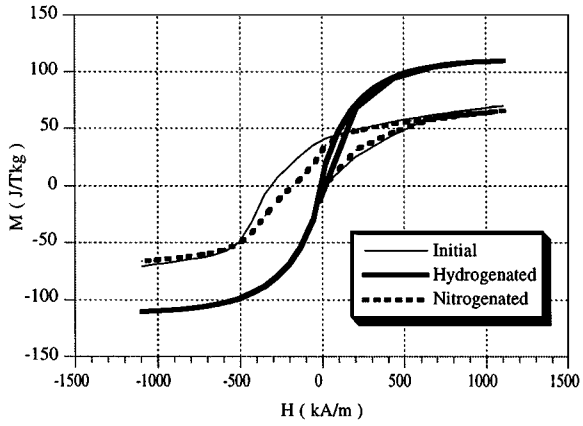

Figure 10 Magnetization curves for the optimally produced initial, hydrogenated, and nitrogenated powders.

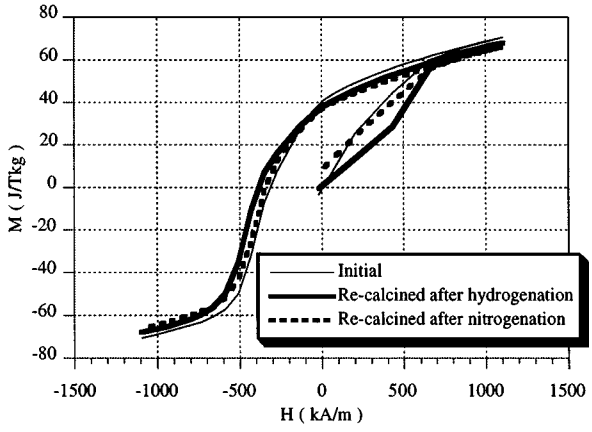

Figure 11 Magnetization curves for the optimally produced initial, hydrogenated and re-calcined, and nitrogenated and re-calcined powders.

variations were much smaller as a result of the very limited reduction of iron oxide to the magnetically softer Fe_3O_4 phase and the absence of Fe.

Fig. 11 shows the comparison between the magnetization curves of these two samples after re-calcination. It is seen clearly that, although the remanence and maximum magnetization of these two samples were very close to those of the initial values, the coercivities were

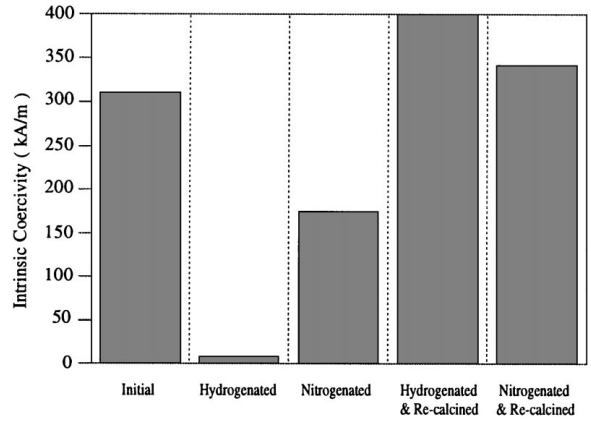

Figure 12 Effects on the intrinsic coercivity of the initial Sr–hexaferrite powder of the optimum gas treatments and re-calcinations.

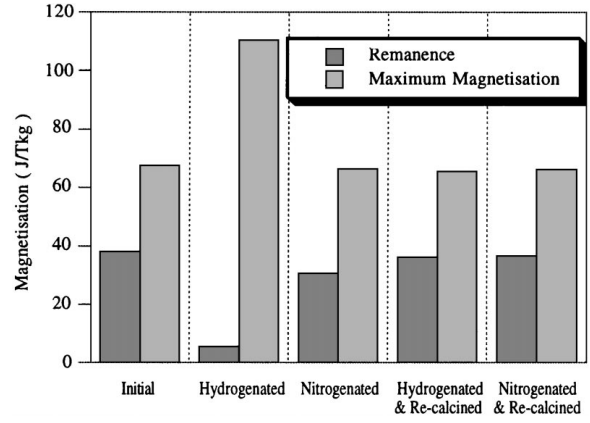

Figure 13 Effects on the remanence and maximum magnetization of the initial Sr–hexaferrite powder of the optimum gas treatments and re-calcinations.

higher and that this increase was more pronounced in the case of the hydrogen processed sample due to its finer structure. The change in the coercivity could also, in part, be due to a change in the anisotropy coefficient (K_1) as result of the composition shift indicated by the lattice parameter changes. The shapes of the initial magnetization curves in Fig. 11 also show that the re-calcined hydrogenated sample exhibited a low initial susceptibility and approached single-domain behavior. However, the nitrogen-processed sample did not give evidence of such behavior.

The comparative magnetic properties of the optimally processed initial, gas-treated (hydrogenation and nitrogenation), plus gas-treated and re-calcined powder samples are summarized in Figs 12 and 13.

Fig. 12 shows the intrinsic coercivities of the powder before and after gas treatment, and after gas treatment and re-calcination. The decrease in the coercive force was much more pronounced in the case of the hydrogenated powder than in the nitrogenated powder. On the other hand, the increase in the coercivities after re-calcination was more appreciable in the hydrogenated powder than in the nitrogenated powder. The highest coercivity obtained was around 400 kA/m (5 kOe).

Fig. 13 indicates the changes in the remanence and maximum magnetization after the gas treatments and re-calcinations. Although these properties were

different than those of the initial sample after hydrogenation and nitrogenation, after re-calcination they showed values very similar to those of the initial powder.

4. Conclusions

During an optimized hydrogen gas heat treatment the Sr–hexaferrite decomposed into $Sr_7Fe_{10}O_{22}$ and Fe_2O_3, with the resultant Fe_2O_3 being reduced to Fe and FeO. In the nitrogen gas heat treatment there was a much lower degree of reduction, which stopped after the formation of Fe_3O_4. The appearance of Fe during the hydrogen treatment resulted in a drastic decrease in the remanence and coercivity and a pronounced increase in the maximum magnetization because of the soft magnetic nature of the Fe. From a microstructural point of view, the initial single-crystal particles changed to particles with a very fine sub-grain structure. However, these changes were observed to be much less marked in the case of the nitrogen treatment owing to the slow reaction kinetics of nitrogen with Sr–hexaferrite. During re-calcination, the reactions reversed, and the hexaferrite phase was re-formed but with a much finer grain size due to fine sub-grain structure formed during the prior gas treatment. The TMA and lattice parameter measurements indicated a compositional shift. The main effect of these changes was on the coercivity, which increased to a value higher than that of the initial powder. This improvement was more appreciable in the case of HTR rather than NTR. The highest coercivity obtained after optimized HTR was ~400 kA/m (5 kOe) compared to the initial value of 310 kA/m (3.9 kOe), while the highest coercivity obtained after optimized NTR was 342 kA/m (4.3 kOe).

Acknowledgements

Thanks are due to the members of the Applied Alloy Chemistry Group (School of Metallurgy and Materials) for their co-operation. The financial support of Tehran University is gratefully acknowledged.

References

1. A. ATAIE, I. R. HARRIS and C. B. PONTON, Patent Application No. PCT/GB95/02758, November 1995.
2. A. ATAIE, C. B. PONTON and I. R. HARRIS, *J. Mat. Sci.* **20** (1996) 5521.
3. S. A. S. EBRAHIMI, A. J. WILLIAMS, N. MARTINEZ, A. ATAIE, A. KIANVASH, C. B. PONTON and I. R. HARRIS, *J. Phys. IV* **7** (1997) C1 325.
4. S. A. S. EBRAHIMI, A. KIANVASH, C. B. PONTON and I. R. HARRIS, *J. Mat. Sci.* **34** (1999) 35–43.
5. *Idem., J. Mat. Sci.* **34** (1999) 45–52.
6. N. MARTINEZ, S. A. S. EBRAHIMI, A. J. WILLIAMS and I. R. HARRIS, *J. Mat. Sci.* (1999) in press.
7. V. ADELSKOLD, *Arkive for Kemi, Min. Geol.* **12A** (1938) 1; JCPDS/24-1207.
8. E. LUCCHINI, D. MINICHELLI and G. SLOCCARI, *J. Am. Ceram. Soc.* **57** (1974) 42; JCPDS/26-980.
9. H. E. SWANSON, NBS Circular 539, **4** (1955) 3; JCPDS/6-0696.
10. T. YAGI, T. SUZUKI and A. AKIMOTO, *J. Geophys. Res.* **90** (1985) 8784; JCPDS/39-1088.
11. National Bureau of Standards, Monograph 25, 5 31, 1967; JCPDS/19-629.
12. L. JAHN and H. G. MULLER, *Phys. Status Solidi* **35** (1969) 723.

Received 19 June
and accepted 6 August 1998